Supplementary data

Suppl. Table 1. NF-L positive amacrine cells in the GCL at P0.
Note: Cells were counted by total NF-L positive cells in the GCL subtracting the number of cells that have distinct RGC pattern. The number of NF-L positive amacrine cells in the wildtype retinas was unable to be objectively counted because of the large number of NF-L positive RGCs masking the possible amacrine cells.

Cell types & Markers	Stage	n	*Wildtype*		*math5*		*math5/brn3b*	
			Average	Std	Average	Std	Average	Std
NF-L Positive cells	P0	4	Not countable	NA	**142.00**	10.86	**75.00**	6.48

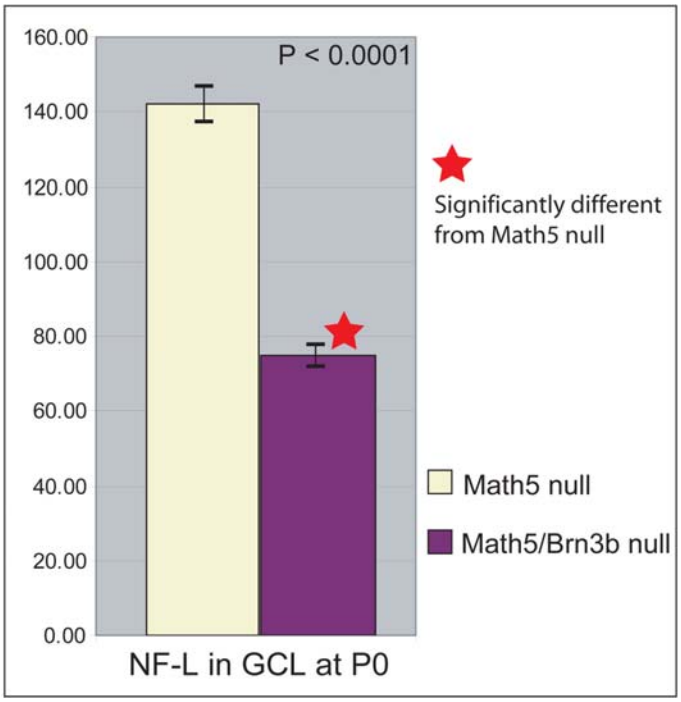

Suppl. Fig. 1. A bar graph representing the number of NF-L positive cells in the GCL. The NF-L positive (presumably amacrine cells) cell number in the Math5/Brn3b-deficient retinas has significant reduction when compared with the Math5-deficient retinas.

Suppl. Table 2. Number of different cell types in the adult retinas (per 150 μm of retinal length)

Cell types & Markers	n	*Wildtype*				*math5*				*math5/brn3b*			
		Average	Std	ratio to INL (%)	Std (%)	Average	Std	ratio to INL (%)	Std (%)	Average	Std	ratio to INL (%)	Std (%)
ONL (PI)	6	**402.33**	42.35	**284.00**	27.00	**386.50**	39.83	**518.00**	144.00	**198.67**	59.80	**420.0**	103.00
INL (PI)	6	**143.17**	28.76	**100.00**	0.00	**78.33**	16.93	**100.00**	0.00	**47.33**	7.34	**100.00**	0.00
Recoverin	6	**5.33**	0.82	**3.76**	0.47	**3.17**	2.99	**4.29**	3.78	**0.83**	1.60	**1.69**	3.27
Pax6	6	**67.50**	9.03	**47.51**	3.19	**47.00**	7.64	**60.96**	8.38	**21.67**	1.75	**46.44**	5.52
ChAT	6	**4.83**	1.47	**3.32**	0.45	**5.83**	1.17	**7.50**	0.94	**4.33**	1.03	**9.12**	1.24
PKC-alpha	6	**36.33**	9.60	**26**	0.08	**27.67**	6.53	**35.32**	4.54	**20.38**	5.00	**41.37**	7.20
Calbindin	6	**1.50**	0.55	**1.03**	0.26	**2.83**	1.33	**3.51**	1.19	**1.17**	1.17	**2.26**	2.21
Sox9	6	**21.83**	1.47	**15.5**	1.67	**23.17**	2.40	**30.17**	3.39	**15.67**	5.20	**35.59**	19.67

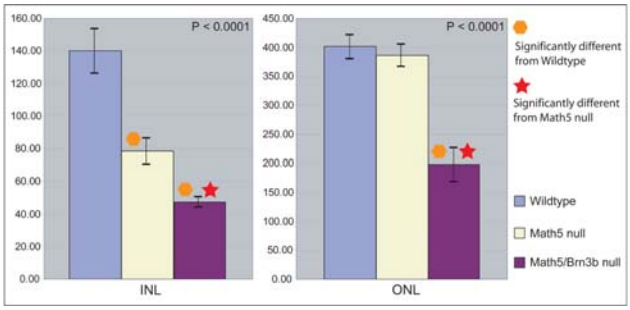

Suppl. Fig. 2. A bar graph showing the cell numbers of radial sectioned adult retinas in the INL and the ONL.

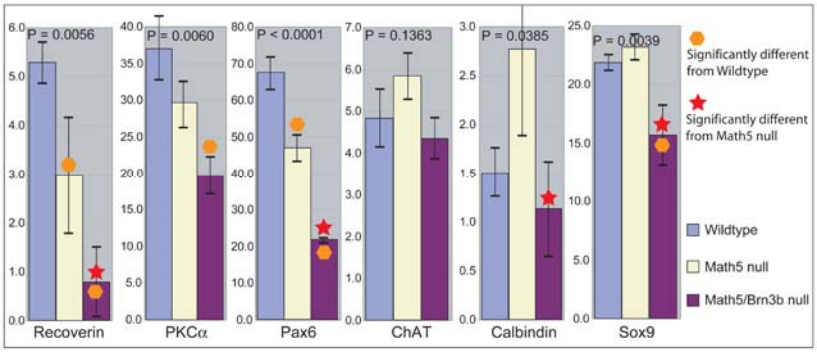

Suppl. Fig. 3. A bar graph showing the cell numbers of radial sectioned adult retinas using different cell markers.

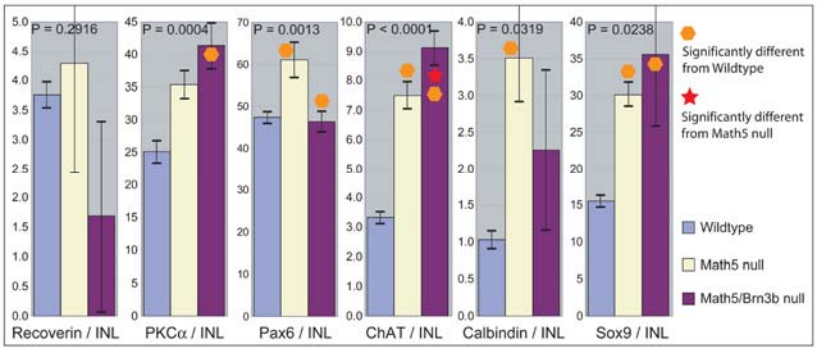

Suppl. Fig. 4. A bar graph showing the ratios of specific cell types to the INL cells. Change of ratio indicates RGC loss having different impacts on different cell types. The average ratio of the recoverin positive cone bipolar cells to the INL cells in the Math5/Br3b-dificient retinas is dramatically reduced. However, no statistical difference was detected. This may be a contribution of the large standard deviation which is resulted from highly uneven distribution of recoverin positive cells.

Suppl. Table 3. Mitotic and Apoptotic cells at E16 and P0.

Cell activity & Markers	Stage	n	*Wildtype*		*math5*		*math5/brn3b*	
			Average	Std	Average	Std	Average	Std
Mitotic cells (PH3)	E16	4	**17.75**	9.00	**58.50**	3.05	**66.25**	13.77
	P0	4	**300.25**	18.39	**244.25**	52.37	**193.00**	18.96
Apoptotic cells (TUNL)	E16	5	**7.40**	2.19	**21.80**	4.44	**19.60**	6.11
	P0	5	**25.20**	4.97	**91.80**	21.51	**127.00**	22.95

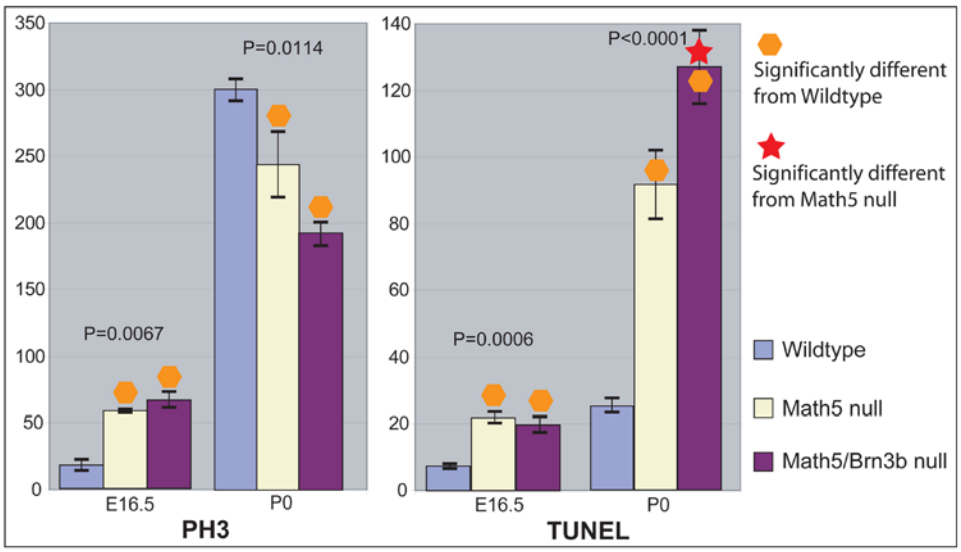

Suppl. Fig. 5. A bar graph representing the counting numbers in Suppl. Table 3.

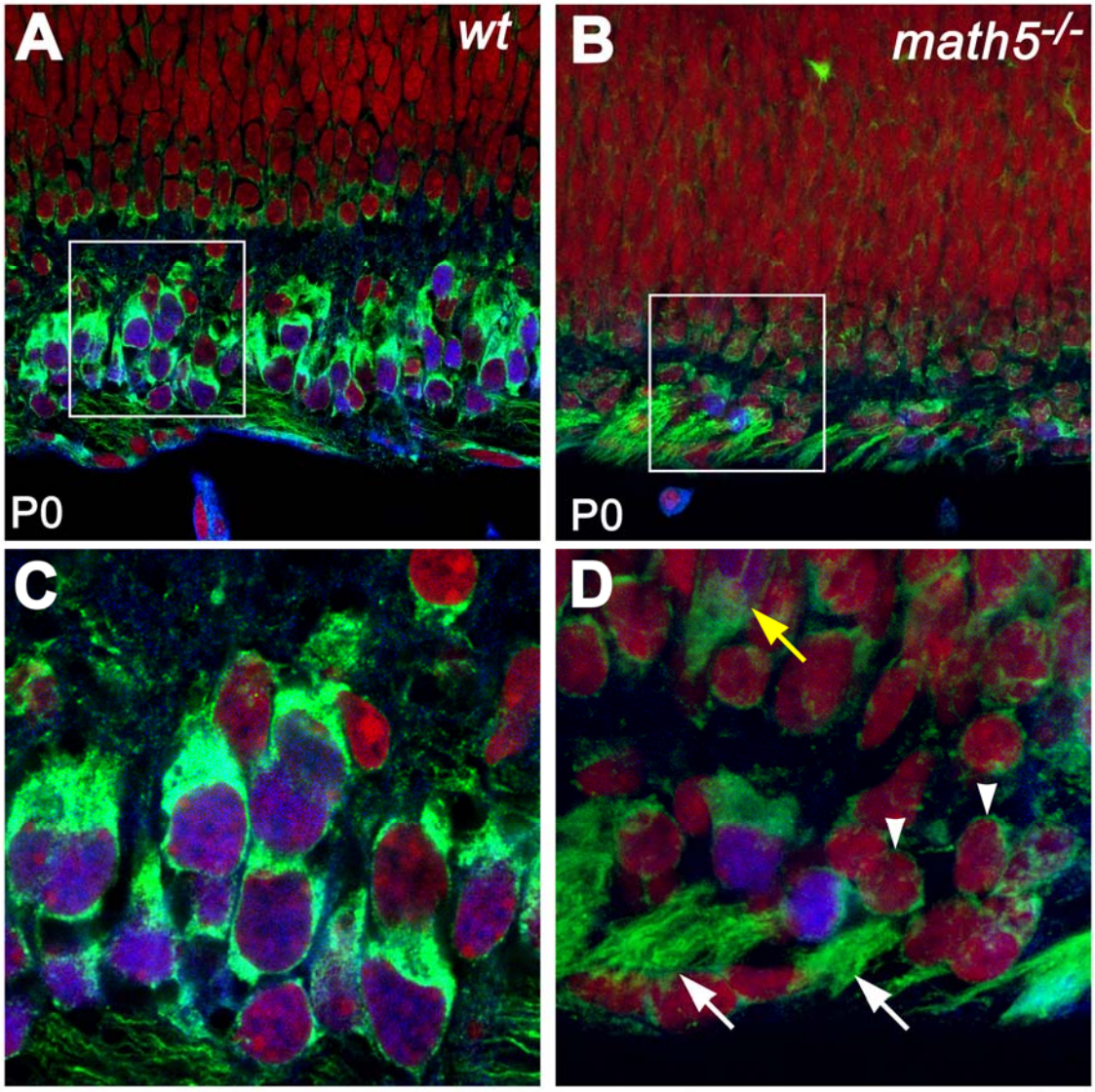

Suppl. Fig. 6. At P0, RGCs exhibit distinct NF-L positive cytoplasmic morphology. In a wildtype retina, most cells in the nascent RGC layer have a prominent NF-L positive cytoplasm facing toward the IPL. These cells are RGCs because they are virtually all positive of Brn3a. Cells with this distinct morphology have drastically reduced in number in the *math5*$^{-/-}$ retina. Cells with thin NF-L positive cytoplasm (arrowheads) filled in the space in the GCL. These cells are most likely amacrine cells because they share the same morphology with the cells in the amacrine cell layer. Although retinas of both genotypes were collected at P0, the *math5*$^{-/-}$ retina was ~8 hrs younger than that of the wildtype. At this stage, cells with RGC characteristics can occasionally be found in the opposite of GCL (yellow arrow). It is likely that these cells are on their way to the GCL. Red: Propidium Iodide; green: NF-L; blue: Brn3a.

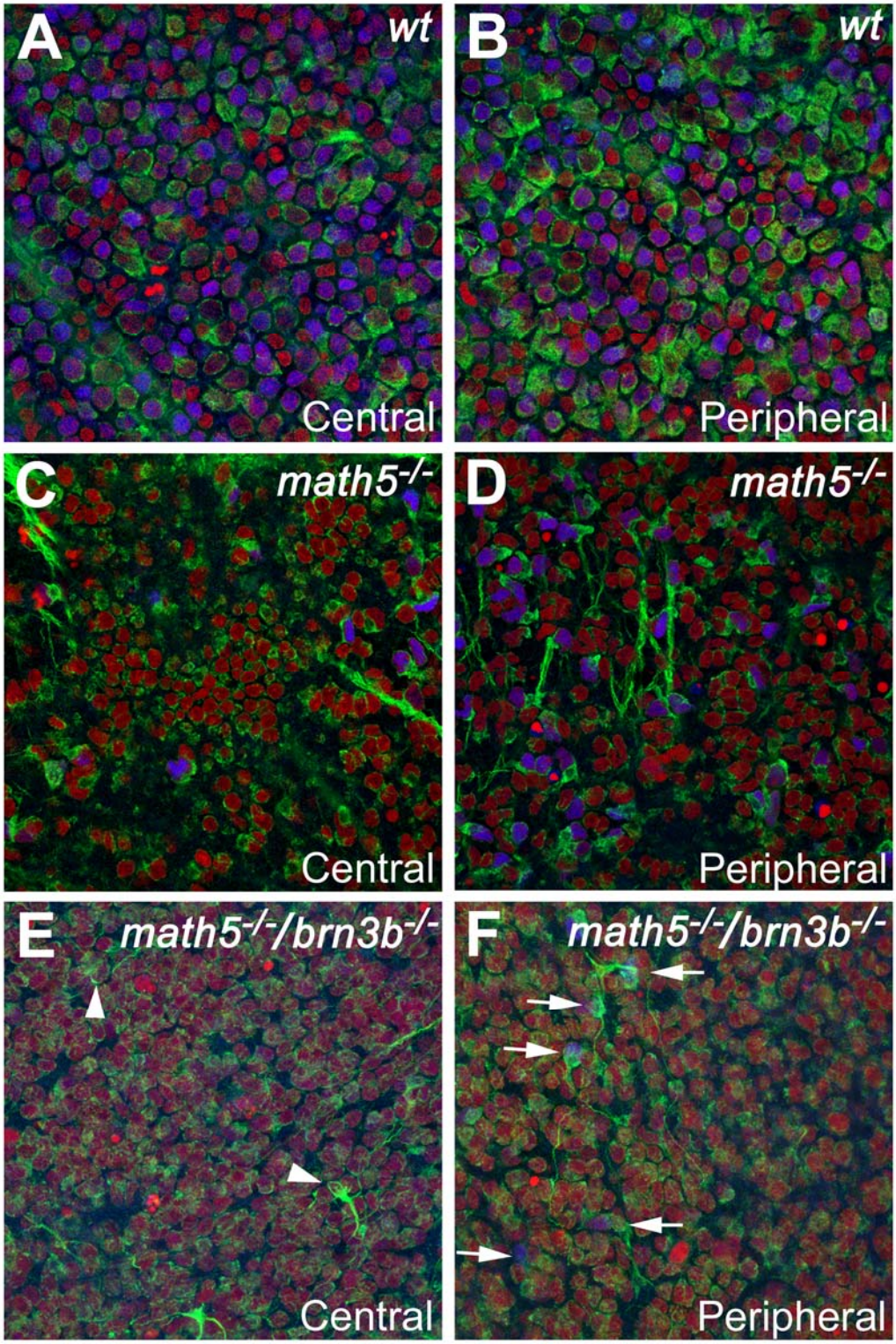

Suppl. Fig. 7. NF-L (green) and Brn3a (blue) positive cells in the flatmounted retinas at P1. Red: propidium iodide. A & B show abundant Brn3a-positive RGCs in both central and peripheral regions of a wildtype retina. C & D show a much higher concentration of Brn3a-positve cells in the peripheral region than in the central region of a *math5*$^{-/-}$ retina. E & F show lacking of Brn3a-positive cells in the central region and rare Brn3a-positive cells in the peripherial region of a *math5*$^{-/-}$*/brn3b*$^{-/-}$ retina. The blue color in E is over enhanced to ensure no positive blue signal escape from visual detection. Speculated Brn3a-negative RGCs in E are indicated with arrowheads. In a *math5*$^{-/-}$*/brn3b*$^{-/-}$ retina, Brn3a-positive cells, that are undetectable in radial sections, can only be seen in the peripheral area (F). These cells (indicated with arrows) have brighter NF-L signal than surrounding amacrine cells. Their axons appear to be misrouted. A, B, C, & D are single optical sections. To ensure no Brn3a-positve cells escape from detection, E & F are projected from 6 optical sections equivalent to 5 μm of thickness.

Suppl. Table 4. The number of Brn3a positive cells in flatmout retinas per 150 μm x 150 μm square.

Cell types & Markers	n	*Wildtype*				*math5*				*math5/brn3b*			
		Average	Std	ratio to PI (%)	Std (%)	Average	Std	ratio to PI (%)	Std (%)	Average	Std	ratio to PI (%)	Std (%)
Brn3a	6	**180.33**	35.19	**53.00**	4.00	**34.67**	16.99	**10.00**	4.00	**3.33**	3.56	**1.00**	1.00
PI: neucleus	6	**338.33**	51.99	**100.00**	0.00	**334.83**	32.71	**100.00**	0.00	**385.50**	61.63	**100.00**	0.00

Note: The images of *math5*$^{-/-}$/*brn3b*$^{-/-}$ retinas used for cell counting are different from those of wildtype and *math5*$^{-/-}$ retinas. For wildtype and *math5*$^{-/-}$ retinas, single optical sections were used. For the *math5*$^{-/-}$/*brn3b*$^{-/-}$ retinas, each image was projected from 6 optical sections equivalent to a thickness of 5 μm. We do so because it is difficult to objectively count the cell numbers when multiple optical sections from wildtype and *math5*$^{-/-}$ retinas were piled. Conversely, we were unable to determine a Brn3a-positive cell if single optical sections from the *math5*$^{-/-}$/*brn3b*$^{-/-}$ retinas were used.

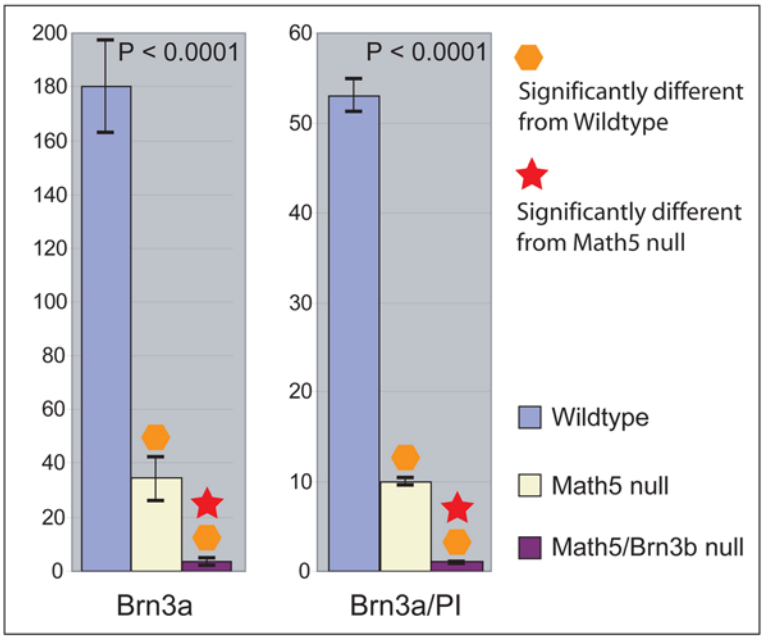

Suppl. Fig. 8. A bar graph representing the counting numbers in Suppl. Table 4.

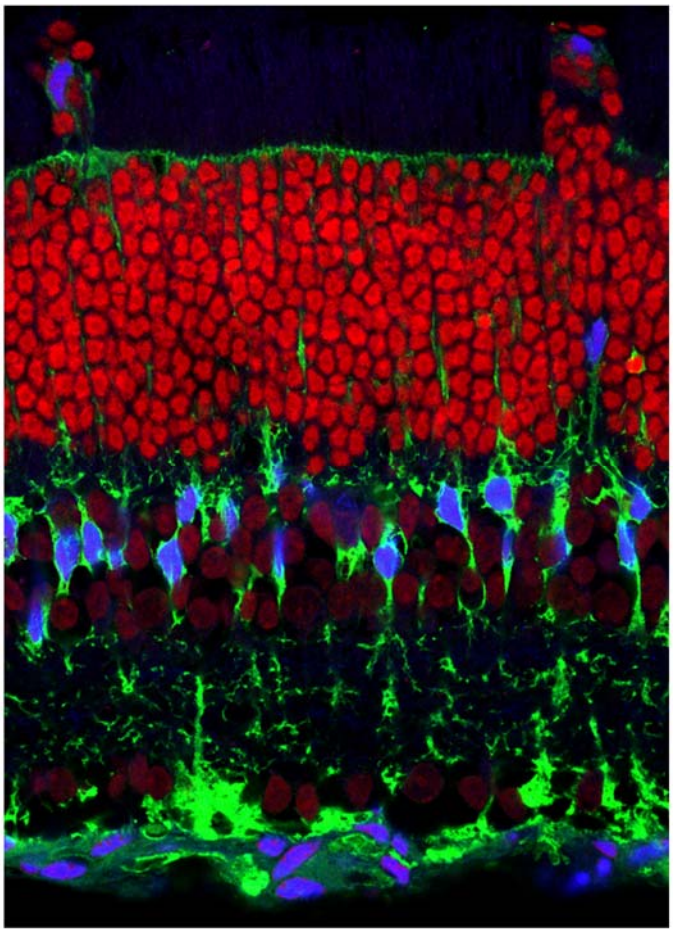

Suppl. Fig. 9. Another example of mis-localized nuclei of Müller glia. In this case, mis-localized Nuclei of Muller glia can be found in every position along the vitreous-ventricular axis including photoreceptor outer segments, ONL and GCL.

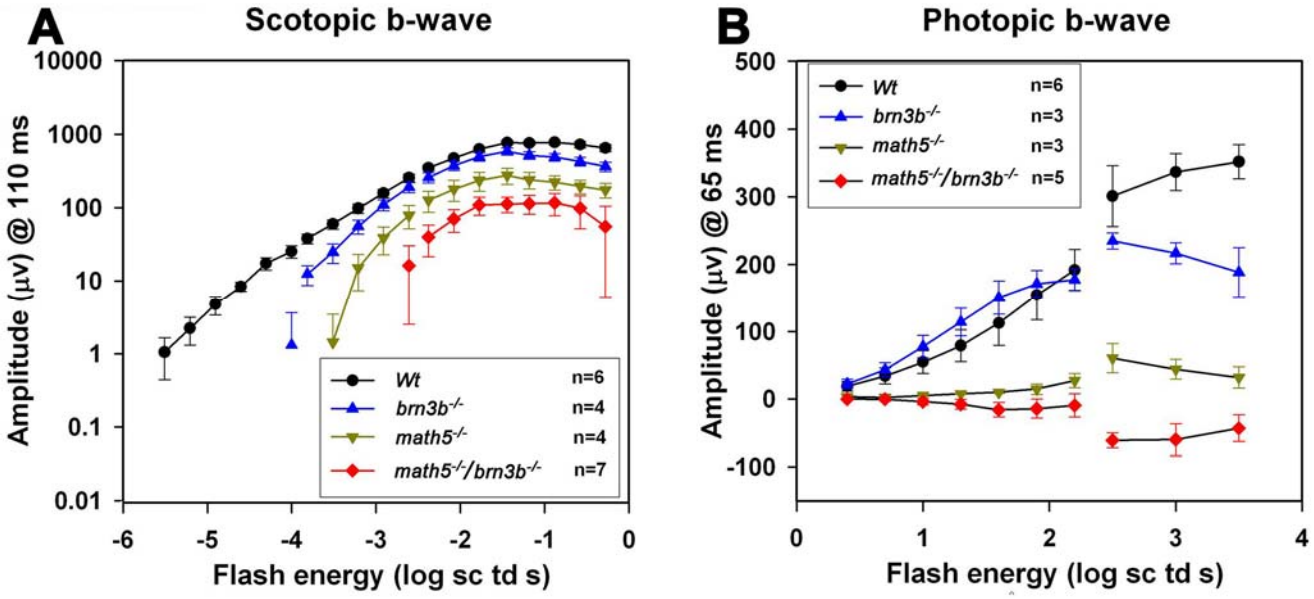

Suppl. Fig. 10. Comparison of ERG b-waves.